George, Mike F.; Annandale, George W.

Bluestone Dam Rock Scour

Bluestone Dam Rock Scour

M. F. George[1], PE and G.W. Annandale[2], D.Ing, PE, D.WRE

[1]Project Geological Engineer, Golder Associates Inc., Lakewood, CO 80227; PH: 303-980-0540; email: Michael_George@Golder.com

[2]Practice / Program Leader, Golder Associates Inc., Lakewood, CO 80227; PH: 303-980-0540; email: George_Annandale@Golder.com

ABSTRACT

Advancements in hydrologic methods have often yielded greater estimates for design flood events. This can be problematic for older dams when the constructed spillway can no longer adequately pass the revised flood estimate. Bluestone Dam is one such case where recent estimates have indicated more than a twofold increase in the design flood magnitude. Moveable bed physical hydraulic model studies for flows greater than the original design indicated complex flow conditions and the potential for significant scour in the unlined hydraulic jump stilling basin. The ability of the homogeneous gravel used in the model study to represent scour potential of intact rock in the actual basin was questionable. As such, Annandale's Erodibility Index Method was used to provide revised scour estimates within the stilling basin. This paper presents a unique solution to a complex problem.

Introduction & Background

Bluestone Dam is a concrete gravity dam located on the New River near Hinton, WV (USA). Built during the 1940's, the dam has a 241 m long spillway with 21 gated overflow spillway bays and 16 lower sluice gates. Flow from the spillway discharges into an unlined hydraulic jump stilling basin (Figure 1). A downstream weir controls the water level within the stilling basin, while baffles on the stilling basin apron and an end sill at the end of the apron are provided to dissipate energy and direct flow upwards before entering the basin. The dam also has six large penstocks (~ 6 m diameter) that can be opened to provide additional discharge capacity.

The spillway was originally designed to pass a probable maximum flood (PMF) event of 12,180 m^3/s while recent advancements in hydrologic methods, however, have indicated more than a twofold increase in the design flood magnitude to 28,320 m^3/s.

Local geology within the stilling basin consists of three main rock types: orthoquartzite, interbedded shale and orthoquartzite, and claystone.

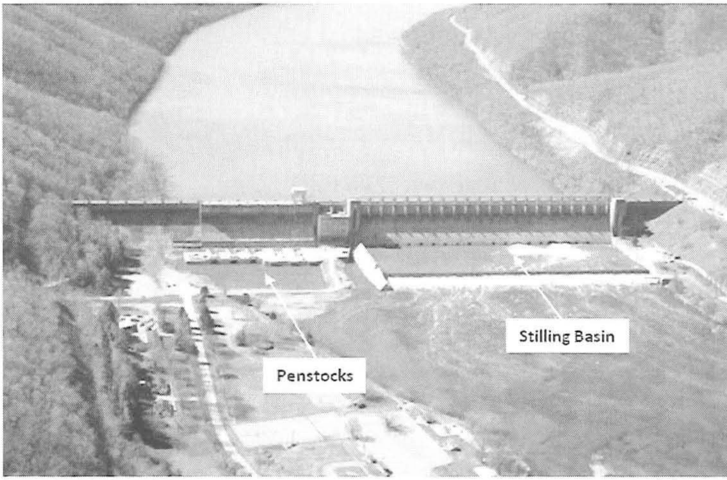

Figure 1. Bluestone Dam layout (Photo courtesy of USACE – Huntington District, Engineering Geology Section).

Physical Hydraulic Model Study

A 1:36 scale physical hydraulic model study was performed to examine scour potential from increased flows beyond the original design discharge up to the revised PMF of 28,320 m^3/s (USACE 2003b). A homogenous gravel bed, consisting of 1 cm size particles, was used to represent rock within the stilling basin.

Based on observation of the video taken of the physical hydraulic model, two main flow conditions exist over the range of discharges analyzed. For discharges up to the original design discharge, the basin functions as designed and a relatively well formed hydraulic jump is witnessed with little to no scour occurring. For the larger discharges, however, flow exiting the spillway into the basin closely resembles that of a "shooting jet". Comparison of the two scenarios is shown in Figure 2.

For the latter scenario, the end sill on the stilling basin apron directs flow upwards (similar to that of a flip bucket), causing the jet to skim on top of the tailwater in the basin and plunge downwards upon impact with the upstream face of the stilling basin weir. Scour-hole formation occurs on the upstream side of the stilling basin weir. Tailwater within the stilling basin is re-circulated forming a large eddy that transports scoured material in the downstream portion of the basin back towards the apron.

Results from the 1:36 scale model indicate a potential for up 27 m of scour within the basin under the revised PMF conditions, which would undoubtedly result in failure of the stilling basin weir. As using gravel to evaluate scour of intact rock in physical model studies may not be representative, it was desirable to attempt to determine how actual rock in the basin would influence scour.

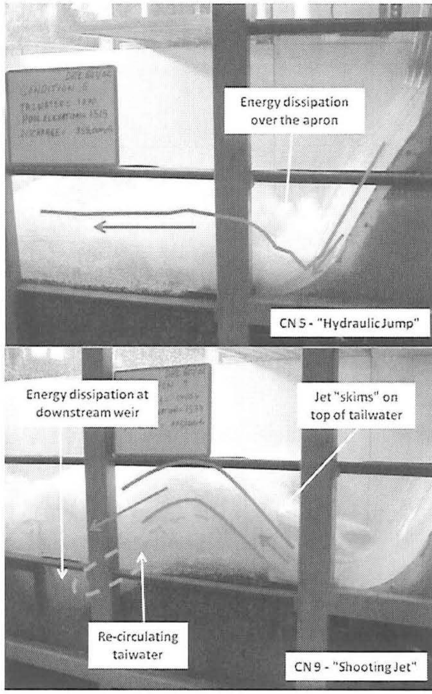

Figure 2. Comparison of flow conditions for discharges less than (top) and greater than (bottom) the original design discharge. Photos courtesy of USACE – Huntington District.

Calibration of Erosive Capacity

For discharges above the original design, flow conditions within the stilling basin are unique, and no one methodology can perfectly represent these conditions. As indicated in Figure 2, higher discharges loosely resemble a shooting jet and therefore jet and plunge pool theories were applied in an attempt to model these distinctive hydraulic conditions with known methods. Figure 3 shows a cross-section of the dam and stilling basin with a schematic of the plunging jet scour module as applied to Bluestone.

The methodology was modified by use of a calibration factor, applied to the calculation of flow erosive capacity within the stilling basin, to account for inadequacies of directly applying the plunging jet module to this flow scenario. Specifically this was done to account for 1) energy dissipation associated with flow through the baffle blocks on the basin apron, 2) the reduction in the jet flow rate applied to the stilling basin floor as an unknown portion of the jet is directed over the stilling basin weir, and 3) energy dissipation associated with jet impinging against the back of the stilling basin weir and being re-directed downwards. The calibration factor was determined through the aid of the 1:36 scale physical hydraulic model.

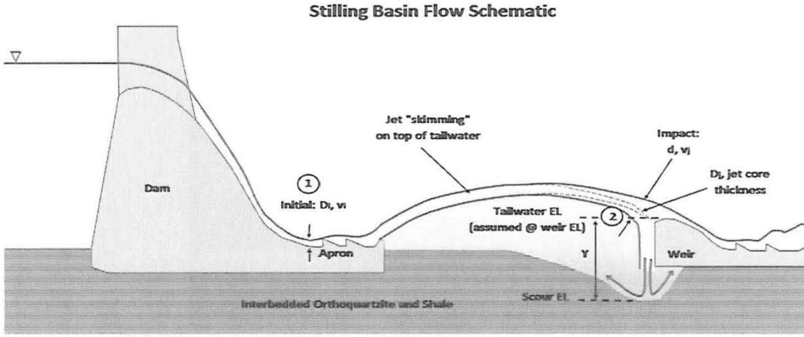

Figure 3. Schematic for shooting jet scenario showing applied plunge pool module (schematic based on typical section from USACE (2003a)).

For theoretical scour predictions, the erosive capacity of the plunging jet (expressed in units of stream power, W/m^2) could be calculated using Annandale's Erodibility Index Method (EIM) (1995, 2006):

$$P_{jet} = \frac{\gamma \cdot Q \cdot H}{A \cdot K} \cdot C_t$$

Where:
γ = unit weight of water (N/m^3).

Q = water discharge (m^3/s).

H = hydraulic head associated with the falling jet (m) taken between locations "1"and "2" on Figure 3.

A = impact area of the jet (i.e., jet footprint) (m^2).

K = factor to calibrate calculated erosive capacity to observed erosive capacity witnessed in the model study (see discussion below).

C_t = total dynamic pressure coefficient (dimensionless) used to determine the relative magnitude of erosive capacity as a function of tailwater depth. Although derived from pressure measurements, use of C_t to portray trends in erosive capacity within the plunge pool quantified by stream power has shown good promise (see George & Annandale 2006a, 2006b, 2008 and Lund et al. 2008). C_t can be expressed as:

$$C_t = C_p + RF \cdot \Gamma \cdot C_p^{'}$$

Where:

C_p = average dynamic pressure coefficient as a function of tailwater depth based on work by Castillo et al. (2007).

Γ = amplification factor to account for resonance that may occur in close-ended rock fissures as a function of tailwater depth (Bollaert 2002). Note that $\Gamma = 1$ (i.e., no amplification) for the calibration with physical model results (as the bed material is gravel) as well as for the theoretical scour calculations as characteristic frequencies for orthoquartzite and shale rock fissures were found not to be within the frequency range of major pressure fluctuations.

RF = unit reduction factor to account for influence of varying degrees of jet break-up based on work by Ervine et al. (1997).

C'_p = fluctuating dynamic pressure coefficient as a function of tailwater depth based on work by Bollaert (2002).

To calibrate the calculated erosive capacity with the erosive capacity observed in the 1:36 scale physical hydraulic model, the calibration factor, K, was adjusted such that the theoretical scour depth matched the observed scour depth in model (Figure 4). Doing so required knowledge of the prototype erosion resistance of the gravel used in the physical model. This is discussed in the following section.

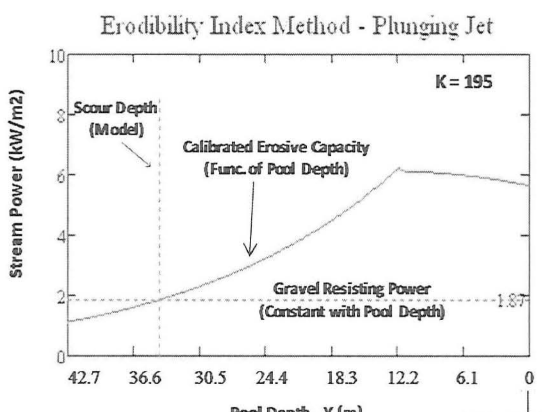

Figure 4. Example of erosive capacity calibration for revised PMF discharge.

Material Resistance

For the calibration, the erosion resistance provided by the gravel in the physical model study could be determined from the critical shear resistance calculated using the Shields parameter (1936) for cohesionless materials.

$$\tau_c = \theta_c \cdot (\rho_s - \rho) \cdot g \cdot d$$

Where:

θ_c = critical Shields parameter for rough turbulent flow = 0.06 (dimensionless).

ρ_s = particle density (kg/m^3).

ρ = water density (kg/m^3).

g = acceleration due to gravity (m/s^2).

d = diameter of gravel used in physical model = 0.01 m.

Using the scale law for stream power between model and prototype, the prototype resisting power of the gravel could be calculated using the following equation from Annandale (2006):

$$P_{cp} = 7.853 \cdot \rho \cdot \left(\sqrt{\frac{\tau_c}{\rho}} \right)^3 \cdot L_s^{\frac{3}{2}}$$

Where:

L_s = model scale = 36 (dimensionless). This value is raised to an exponent of three-halves to covert from model resisting power to prototype resisting power.

Once the calculated erosive capacity has been calibrated with the model scour results (based on the prototype resisting power of the gravel), the actual rock resistance can be inserted into the plunge pool scour module to determine a revised estimate for scour depth. Rock erodibility can be determined using the EIM (Annandale, 1995): The erodibility index, K_h, can be defined as:

$$K_h = M_s \cdot K_b \cdot K_d \cdot J_s$$

Where:

M_s = mass strength number.

K_b = block/particle size number. For rock, K_b = RQD/J_n, where RQD is the rock quality designation and J_n is the joint set number.

K_d = discontinuity/interparticle bond shear strength number. For rock, $K_d = J_r/J_a$, where J_r is the joint roughness number and J_a is the joint alteration number.

J_s = relative ground structure number.

The critical resisting stream power, P_c (W/m^2), of rock materials may be quantified using the following equation from Annandale (2006):

$$P_c = 1000 \cdot K_h^{0.75}$$

As stated above, three main rock types are found within the stilling basin: orthoquartzite, interbedded shale and orthoquartzite, and claystone. The more massive orthoquartzite layers are classified as hard to very hard rock and were determined to have a relatively high resistance to erosion. Conversely, shale layers are classified as soft to very soft rock and were found to have a relatively low erosion resistance. As indicated in Figure 5, the size of individual shale blocks is considerably smaller than those of the massive orthoquartzite units, contributing further to the difference in capacity to resist erosion. Although orthoquartzite layers are found interbedded with shale, these layers are likely to be undermined by erosion of the surrounding shale material. Subsequently, erosion resistance for the interbedded material as a whole was solely based on geologic properties for the shale.

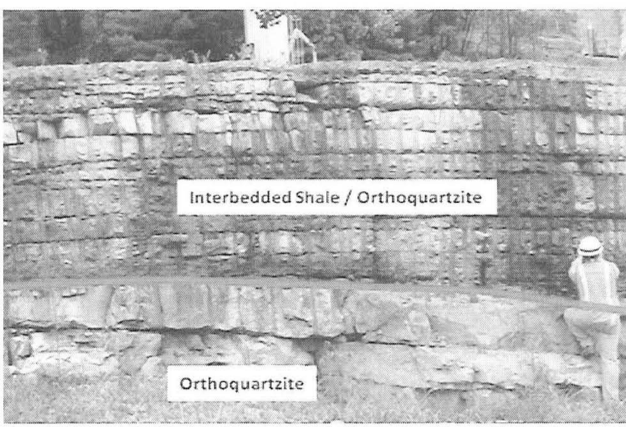

Figure 5. Outcrop at Bluestone Dam showing contact between massive orthoquartzite (bottom) and interbedded shale / orthoquartzite (top). Photo courtesy of USACE – Huntington District, Engineering Geology Section).

Claystone material resistance is less than that of the massive orthoquartzite but greater than the interbedded material. Claystone is only encountered approximately 20 m to 33 m below the stilling basin floor. Table 1 shows the calculated high and low resisting powers provided by the different rock types as well as for the gravel in the physical model study.

Table 1. Material resisting power

Rock Formation	Erodibility Index		Resisting Power (kW/m2)	
	High	*Low*	*High*	*Low*
Orthoquartzite	1199	178	204	49
Interbedded Orthoquartzite / Shale	2.24	0.47	1.83	0.57
Claystone	204	43	54	17
1:36 Scale Model Gravel (Prototype)	2.30		1.87	

Rock Scour Prediction Results

Comparison of calibrated erosive capacity for the shooting jet with the actual rock resistance yielded revised estimates of scour depth in the stilling basin. Figure 6 shows interpreted scour profiles for different discharges above the original design discharge up to the revised PMF (indicated by conditions (CN) 7 – 11) for a typical cross-section through one of the dam monoliths.

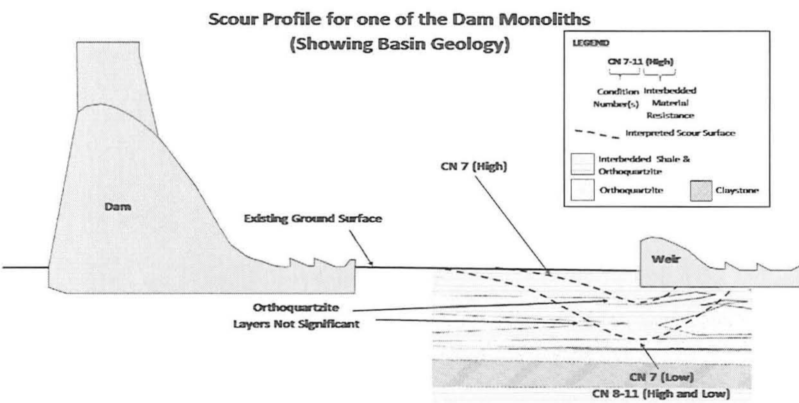

Figure 6. Scour results for typical section (Note profiles are interpreted; only the maximum depth is calculated). Geology and typical section from USACE (2003a).

For all flows analyzed, only interbedded shale material could be eroded. As indicated in Figure 6, layers of intact orthoquartzite exist, however, if these layers were not of sufficient thickness (i.e., approximately 1 m to 2 m), they were considered capable of being eroded by being undermined.

Note that the high resisting power of the interbedded shale (1.83 kW/m^2) is nearly identical to the prototype resisting power provided by the gravel (1.87 kW/m^2), which this suggests that the scour depths witnessed in the physical model could be relatively accurate for actual conditions. Should interbedded shale resistance be closer to the low value (0.57 kW/m^2), scour depths could be deeper than those predicted by the physical model.

Figure 7 shows the different values obtained for the calibration factor, *K*, applied to the calculated erosive capacity for varying discharges above the original design. As indicated, the calibration factor begins to decrease rapidly for increasing discharge. This suggests two potential conclusions 1) more energy is dissipated for lower flows, and 2) higher flows are better represented by the plunging jet module. Values of *K* for all flows above the original design discharge are relatively high (i.e., between 95 and 245) indicating a significant amount of erosive capacity is lost. As mentioned above, this could potentially be attributed to a reduction in discharge from an unknown amount of flow in the jet going over the stilling basin weir or energy being dissipated from flow impacting apron baffles and the upstream side of the stilling basin weir.

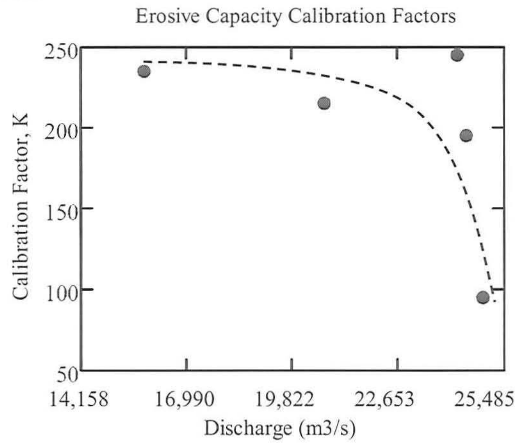

Figure 7. Erosive capacity calibration factors based on 1:36 scale hydraulic model.

Conclusions and Discussion

Flow conditions for discharges above the original design discharge in the Bluestone Dam stilling basin are unique, but loosely akin to a shooting jet into a plunge pool. As such, jet and plunge pool theories were applied in conjunction with physical hydraulic model study results to determine representative rock scour estimates for flows within the stilling.

Based on the results of the analysis, scour depths within the stilling basin can likely be equal to or greater than those witnessed in the physical model. The theoretical depths calculated are deemed to be the most representative of actual scour conditions likely to exist as the actual rock resistance was incorporated using Annandale's EIM.

The analysis was not without limitation. Most significantly, it was assumed that the scour-hole geometry (and subsequently the erosive capacity within the pool) for the gravel material in the physical hydraulic model would be similar to that formed in the rock in the actual stilling basin. In actuality, because the materials are different, it would be reasonable to assume scour-hole shapes would different with dissimilar flow patterns and ultimately varying erosive capacities.

In spite of this, it is felt that the above methodology provides a reasonable and representative solution to a scour problem with unique and complex hydraulic flow conditions.

Acknowledgements

The authors would like to thank Mr. Michael McCray and Mr. Stephen Spoor (USACE – Huntington District) as well as Mr. Jeffery Dingrando (Stantec) for their collaboration on the project and their cooperation with this paper.

References

Annandale, G.W. (2006). *Scour Technology*. New York, McGraw-Hill.

Annandale, G.W. (1995). "Erodibility." *J. Hyd. Res.* 33, 471-494.

Bollaert, E. (2002). Transient Water Pressures in Joints and Formation of Rock Scour due to High-Velocity Jet Impact, *PhD Thesis: Communication 13*, Laboratory of Hydraulic Constructions, Swiss Federal Institute of Technology, Lausanne, Switzerland.

Castillo, L.G., Puertas, J. and J. Dolz. (2007). Contribution to discussion of Bollaert and Schleiss' paper "Scour of rock due to the impact of plunging jet Part 1: A state-of-the-art review". *J. Hyd. Res.* 45, 853-858.

Ervine, D.A., H.T. Falvey, and W. Withers. (1997). "Pressure Fluctuations on Plunge Pool Floors". *J. Hyd. Res.* 35, 257-279.

George, M. F. and G. W. Annandale. (2006a). "Kariba Dam Plunge Pool Scour." *Proc., 3rd Int. Conf. on Scour and Erosion*, Amsterdam, Netherlands.

George, M. F. and G. W. Annandale. (2006b). "Dam Failure by Rock Scour: Evaluation & Prevention (A Case Study)." *Proc., 41st U.S. Rock Mechanics Symposium (GoldenRocks 2006)*, Golden, CO, USA.

George, M. F. and G. W. Annandale. (2008). "Decreasing Scour Potential Downstream of Overtopping Dams Using Crest Modifications." *Proc., 4th Int. Conf. on Scour and Erosion*. Tokyo, Japan.

Lund, G., M. F. George, H. T. Falvey, G. W. Annandale and D. Lopez. (2008). "Eagle Nest Dam: Hydraulic Model Study of Flood Overtopping." *Proc., Conf. on Dam Safety*, ASDSO, Palm Springs, CA, USA.

Shields, A. (1936). "Anwendung der Aehnlichkeitsmechanik und der Turbulenz Forschung auf die Geschiebebewegung". Mitt. der Preussische Versuchanstalt für Wasserbau und Schiffbau, Berlin, Germany, No. 26.

United States Army Corps of Engineers (USACE) Huntington District. (2003a). "Appendix A" *Bluestone Dam Design Document Report (DDR).*

United States Army Corps of Engineers (USACE) Huntington District. (2003b). "Appendix B: Hydrology & Hydraulics, Annex B – Bluestone Lake Dam, Baffle Blocks and Tailrace Study." *Bluestone Dam Design Document Report (DDR).*